

Ionic conductivity measurements of molten iodide-based electrolytes

Patrick Masset^{a,b,c,*}, Antoine Henry^a, Jean-Yves Poinso^{a,1}, Jean-Claude Poignet^c

^a CEA Le Ripault, BP 16, 37260 Monts, France

^b ASB-Aerospatiale Batteries, Allée Saint-Hélène, 18021 Bourges, France

^c LEPMI, BP 75, 38402 Saint-Martin d'Hères, France

Received 4 December 2005; received in revised form 4 January 2006; accepted 4 January 2006

Available online 17 February 2006

Abstract

A number of iodide-based electrolytes (LiCl–LiI, LiI–KI, LiCl–LiBr–LiI, LiCl–LiI–KI and LiF–LiCl–LiI) were considered to be used in thermal batteries. Ionic conductivity of multi-cation and all-lithium electrolytes were evaluated. They were compared to the classical electrolytes (LiCl–KCl, LiF–LiBr–KBr and LiF–LiCl–LiBr) used in thermal battery applications. Measurements were realised by electrochemical impedance spectroscopy (E.I.S.). It was shown that some all-lithium iodide-based electrolytes exhibit interesting ionic conductivities and are suitable as electrolytes in thermal batteries. It was pointed out that activation energy E_a was close to 11 kJ mol^{-1} for multi-cation electrolytes, whereas it was equal to 7 kJ mol^{-1} for all-lithium electrolytes.

© 2006 Elsevier B.V. All rights reserved.

Keywords: Molten salt; Ionic conductivity; Iodides; Electrolytes; Thermal batteries

1. Introduction

Thermal activated batteries are suitable electrical generators for military applications [1] due to their reliability and robustness. Installed on the dedicated devices, they can remain more than 20 years without performance degradation. Electrical needs increase more and more, especially for long time operations. To reach the future performance requirements, various improvements are under investigation. The performance benefits expected from a temperature increase in the initial stage are rather limited by the thermal decomposition of pyrite (see the Fe–S phase diagram [2,3] and experimental studies under helium atmosphere [4,5] and in molten salts [6]). In this frame, iodide-based electrolytes were investigated. Molten iodide mixtures present low melting points (m.p.) compared to the chloride, bromide or fluoride-based mixtures. Thus, a global performance improvement is expected from their use. In the past, iodide-based electrolytes have been envisaged and abandoned for three reasons:

- (i) The relative high cost of lithium iodide LiI in comparison to other lithium halides [7].
- (ii) Iodide salts are very hygroscopic [8] and water up-take kinetic is unfavourable compared to other halides [8,9], therefore, a careful drying must be performed in order to avoid hydrolysis [10].
- (iii) Lithium iodide forms easily low temperature hydrates with water which are stable at highest temperatures [12,13] compared to other lithium halides LiCl [13–16] or LiBr [13–15].

Earlier, our group reported [11] partial results based on ionic conductivity measurements of iodide-based electrolytes. At the meantime, Guidotti and Reinhardt [17] published results showing that iodide-based electrolytes (LiF–LiCl–LiI ternary eutectic and LiF–LiCl–LiBr–LiI: two quaternary compositions) are attractive electrolytes for thermal batteries. The quaternary LiF–LiCl–LiBr–LiI (15.4–21.7–32.9–30 mol%) has already been studied by Borger et al. [7] for high temperature batteries. In molten salt electrolytes, the “current” transportation through single cells is ensured by ionic species migration. Usually, the mobility follows Arrhenius-type behaviour. The resulting ionic conductivity is then equal to:

$$\kappa = \kappa^{\circ} \exp\left(\frac{-E_a}{RT}\right) \quad (1)$$

* Corresponding author. Present address: Karl Winnacker Institut der Dechema e.V., Theodor-Heuss Allee 25, 60486 Frankfurt am Main, Germany. Tel.: +49 69 7564 362; fax: +49 69 7564 388.

E-mail address: masset@dechema.de (P. Masset).

¹ Present address: CEA Valduc, 21120 Is-sur-Tille, France.

Table 1
Melting point and composition of the molten salt electrolytes used in this study

Salts	Melting point (°C)	Mass fraction (mass%)	Molar fraction (mol%)	References
LiCl–LiI	368	34.6–65.4	14.4–85.6	[24]
LiI–KI	285	58.2–41.8	63.3–36.7	[25,26]
LiCl–LiI–KI	265	8.5–59–32	2.6–57.3–40.1	[27]
LiF–LiCl–LiI	341	3.2–13–83.8	11.7–29.1–59.2	[28]
LiBr–LiCl–LiI	368	16.07–10.04–73.88	19–24.3–56.7	[24]
LiCl–KCl	354	44.8–55.2	58.8–41.2	[24]
LiF–LiCl–LiBr	443	9.6–22–68.4	22–31–47	[29]
LiF–LiBr–KBr	323	0.67–53.5–45.83	2.5–60–37.5	[9]
	323	0.81–56–43.18	3–63–34	[18]
LiCl–LiBr–KBr	313	12–36.6–51.4	25–37–38	[24]

where κ° is the pre-exponential factor, E_a the activation energy, R the gas constant ($R = 8.3145 \text{ J mol}^{-1} \text{ K}^{-1}$) and T is the absolute temperature. Moreover, in thermal batteries, due to the high level of mechanical stresses (acceleration, gyration, ...), the electrolyte needs to be immobilised by a binder. It constitutes the so-called “separator”. Usually, the binder is made of metallic oxides such as silica, alumina or magnesia powders which are electrical insulators. Redey et al. [18] measured the ionic conductivities of retained electrolytes (LiCl–KCl, LiCl–LiBr–KBr, LiF–LiCl–LiBr, LiF–LiBr–KBr). They expressed the ionic conductivity of the separator as follows:

$$\kappa = \kappa^\circ \exp\left(\frac{-E_a}{RT}\right) \psi_{\text{MgO}}^\alpha \quad (2)$$

The parameter ψ_{MgO} represents the weight fraction of magnesia MgO and the parameter α depends on the electrolyte nature. The free volume remaining after the pelletisation step modifies significantly the ionic conductivity of the separator [19]. Recently, in the course of this project, we showed [20] that a constant volume fraction of binder was relevant whatever the nature of the electrolyte. In the literature, only a few data are available. Ionic conductivities of binary mixtures (LiCl–LiI and LiI–KI) were analysed by Janz [21]. To our knowledge, there were no data published of the ionic conductivity of the LiF–LiCl–LiI ternary mixture, except one value. The value of 2.3 S cm^{-1} at 375°C (648 K) was given for the LiF–LiCl–LiI electrolyte used in Li/S cells [22].

Due to the mixing properties of each component in a given mixture, the resulting ionic conductivity does not simply be described with the sum of the single contributions with regards to their molar fraction. It means that experimental measurements are required for binary and higher order mixtures. The aim of this work is to provide new and accurate ionic conductivity measurements of attractive iodide-based electrolytes (binary and ternary eutectic compositions) to be used in thermal batteries.

2. Experimental

2.1. Materials

The salts LiF, LiCl, LiBr and KBr were supplied from Sigma–Aldrich (+99.99% purity) and lithium iodide LiI (99.9% purity; –200 mesh) from Cerac. The salts were individually dried

under vacuum in a quartz crucible for 15 h at 200°C (473 K). Fluoride-based salts were fused in glassy carbon crucibles to prevent silica dissolution in the salt. Salt mixtures were fused under dry argon, and maintained at 500°C (773 K) for 15 h. They were quenched in the grinder directly. Once ground, they were stored in a glove box under inert atmosphere. Impurity concentrations (mainly oxides and hydroxides) were determined to be less than 10^{-4} molar fraction. In the case of LiI, a molar fraction of 5×10^{-2} was measured. The electrolyte compositions are reported in Table 1. In the literature, for the same LiI–KI eutectic composition, the melting point was 25°C lower in one case [23]. Lithium iodide is known to form easily hydrates with water [8]. It might be envisaged that salts were not dried carefully enough. By means of thermal analysis, the lithium iodide–potassium iodide eutectic melting point was found close to 285°C . Our results are in good agreement with the data published by Johnson and co-workers [26] and later confirmed by Sangster and Pelton [24].

2.1.1. Apparatus

The ionic conductivity cell device was made either of quartz or boron nitride (see details in Fig. 1). The BN cell was employed with the fluoride-based salts. In the past, pressed boron nitride has been successfully used as raw material for the design of conductance cell with pure molten fluorides [30,31]. The inner part of the cell contains a capillary which length and internal radius are equal to 30 and 3 mm, respectively. The outer part of the apparatus is a stainless steel container which plays the role of inert electrode. Its inner diameter is adjusted to the outer one of the BN part at high temperature. It takes into account the difference of thermal expansion coefficients between BN (or quartz) and stainless steel. A second inert electrode is disposed at the other extremity of the capillary filled with the molten salt. As the properties of the LiCl–KCl eutectic are now well established, the apparatus was first tested with this eutectic mixture. The preliminary results obtained with the LiCl–KCl mixture are in agreement with the literature data within less than 5% [21].

2.2. Experimental protocole

Ionic conductivity measurements were realised by electrochemical impedance spectroscopy (E.I.S.). From an electrical point of view, the small capillary filled with the molten salt acts

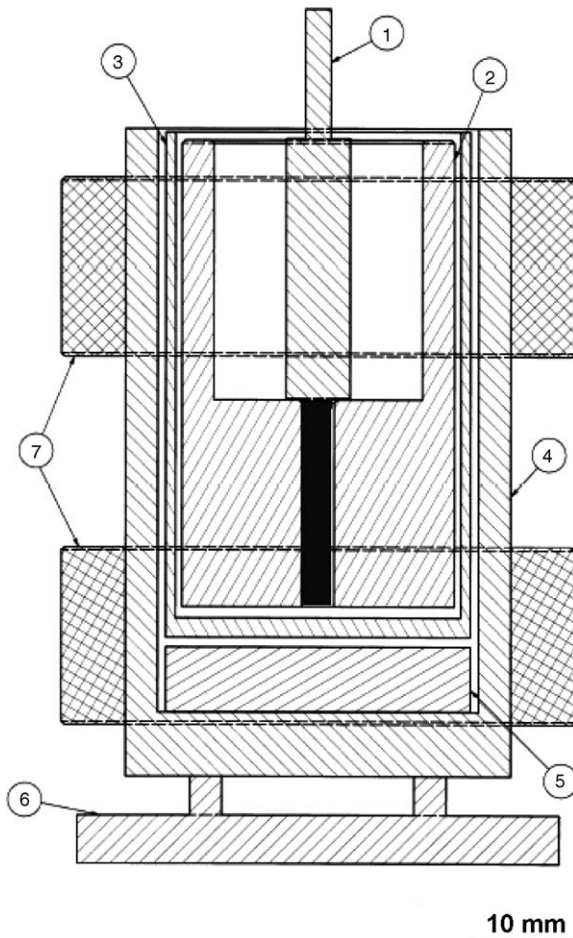


Fig. 1. Apparatus used for ionic conductivity measurements situated in a glove box: (1) upper electrode, (2) BN or quartz cell with capillary, (3) lower electrode, (4) oven made of copper, (5) insulates, (6) support, (7) heating coil and (■) molten salt.

as a pure resistance. The impedance caused by the molten salt can be calculated as follows:

$$Z(t) = \frac{E(t)}{I(t)} \quad (3)$$

where $E(t) = E_0 e^{j\omega t}$ and $i(t) = I_0 e^{j(\omega t + \phi)}$. $E(t)$ is the imposed input signal and $I(t)$ is the measured output signal. The resistance was taken when the imaginary part of the impedance was equal to zero:

$$R_\epsilon = \lim_{Z''(w) \rightarrow 0} Z'(w) \quad (4)$$

The ionic conductivity κ is equal to:

$$\kappa = \frac{1}{R_\epsilon} \frac{l}{S} \quad (5)$$

where l and S represent the length and the section area of the capillary, respectively. Each experiment was repeated at least five times and an average value was given. Measurements started at the melting point of the mixture. Each 50 °C (400, 450, 500 °C, ...), measurements were carried out during the heating cycle. Once the thermal equilibrium was reached (usually, within less than 1 h), the measurements were performed. The same procedure was repeated during the cooling step. The first temperature

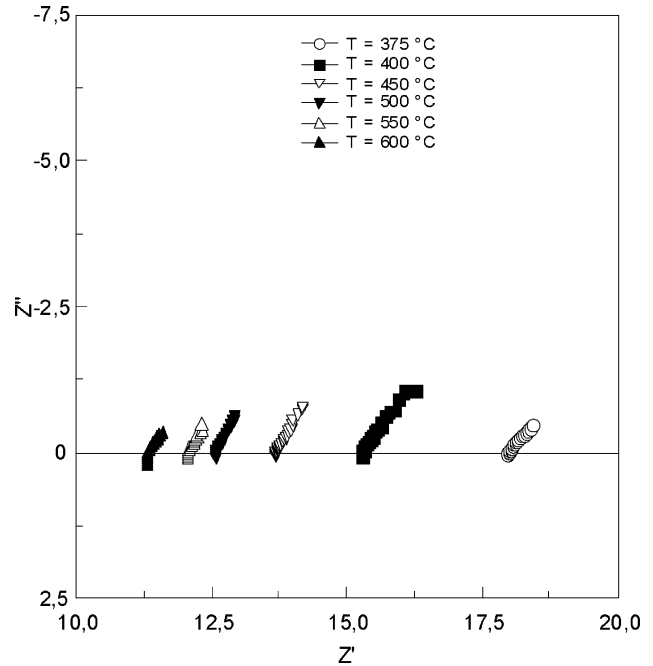


Fig. 2. Typical $-Z''(\Omega) = f(Z'(\Omega))$ Nyquist diagram evolution with temperature obtained for the LiF–LiCl–LiI electrolyte.

was shifted by 25 °C and experiments were carried out at 575, 525, 475 °C, ... Using this procedure, the molten salt stability was also checked during the experiments.

3. Results and discussion

3.1. Reproducibility and accuracy of the measurements

Fig. 2 sketches a typical Nyquist diagram $-Z''(w)$ versus $Z'(w)$ obtained with the LiF–LiCl–LiI electrolyte at between 375 and 600 °C. The measured resistance varies from 10 to 20 Ω. The relative error was calculated with the following equation:

$$\frac{\Delta\kappa}{\kappa} = 2 \frac{\Delta r}{r} + \frac{\Delta l}{l} + \frac{\Delta R_\epsilon}{R_\epsilon} \quad (6)$$

Δr and Δl are the radius and length variations, respectively. It is mainly due to the thermal expansion of materials with temperature. The quartz or boron nitride dilatation with the temperature was considered as negligible [32]. Therefore, the resistance uncertainty was mainly correlated to temperature oscillations around the consign temperature (Eq. (7)). Its variation, estimated to be close to 0.05 Ω, was obtained with five measurements (Fig. 3). The relative error was estimated to be less than 5% with our apparatus:

$$\frac{\Delta\kappa}{\kappa} = \frac{\Delta R_\epsilon}{R_\epsilon} \quad (7)$$

3.2. Ionic conductivity evolution versus the temperature

The ionic conductivities of different electrolytes were measured with temperature by E.I.S. For all-lithium electrolytes

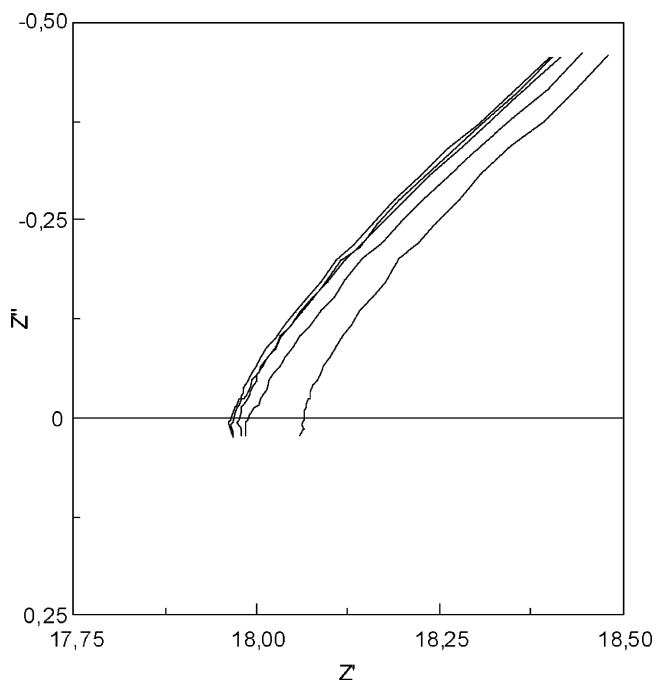


Fig. 3. Typical- $Z''(\Omega) = f(Z'(\Omega))$ Nyquist diagram evolution at 375 °C (648 K) with temperature obtained for the LiF-LiCl-LiI electrolyte.

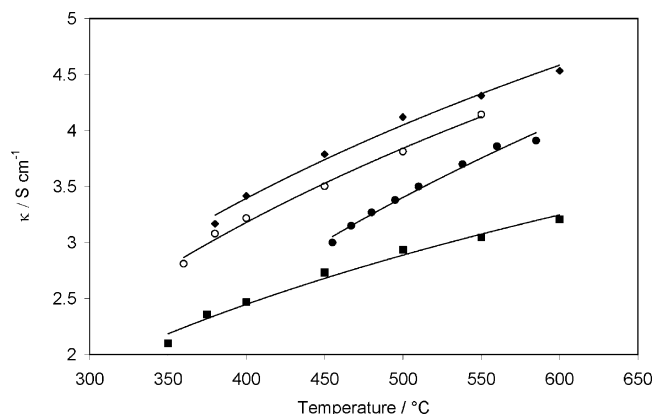


Fig. 4. Evolution of the ionic conductivity vs. the temperature of all-lithium electrolytes: (◆) LiCl-LiI, (○) LiCl-LiBr-LiI, (●) LiF-LiCl-LiBr and (■) LiF-LiCl-LiI.

Table 2
Analytical expressions of ionic conductivity of electrolytes measured in this work

Electrolyte	Composition (mol%)	Ionic conductivity ($S\text{ cm}^{-1}$)
LiCl-LiI	36.4–65.4	$13.0462 \exp(-907.3/T(K))$
LiI-KI	63.3–36.7	$10.0001 \exp(-1387.9/T(K))$
LiCl-LiI-KI	8.5–59–32	$11.0055 \exp(-1329.4/T(K))$
LiF-LiCl-LiI	11.7–29.1–59.2	$8.895 \exp(-872.6/T(K))$
LiBr-LiCl-LiI	19–24.3–56.7	$12.6746 \exp(-925.0/T(K))$
LiCl-KCl	58.8–42.1	$18.7876 \exp(-1800.6/T(K))$
LiF-LiCl-LiBr	22–31–47	$17.8664 \exp(-1284.24/T(K))$
LiF-LiBr-KBr	0.67–53.5–45.83	$20.5817 \exp(-1944.76/T(K))$
LiCl-LiBr-KBr	12–36.6–51.4	$14.1221 \exp(-1884.66/T(K))$

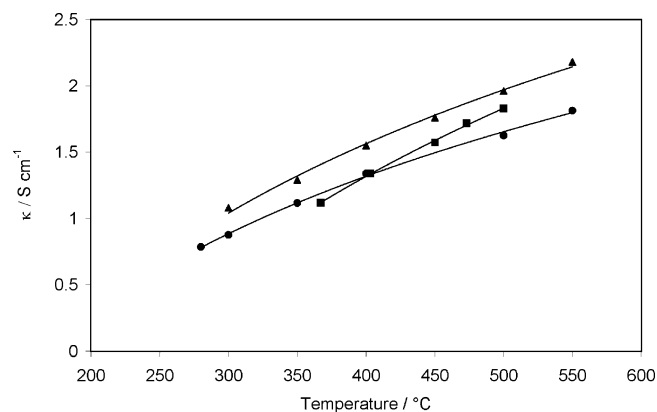


Fig. 5. Evolution of the ionic conductivity vs. the temperature of all mixed cation electrolytes: (▲) LiCl-LiI-KI, (■) LiCl-KCl and (●) LiI-KI.

(containing only lithium cation), the ionic conductivity values range between 2 and 4.5 S cm^{-1} (Fig. 4). The ionic conductivities of multi-cation electrolytes were found to be smaller (Fig. 5). Values range between 0.7 and 2 S cm^{-1} . The analytical expressions of the conductivities measured in this work are reported in Table 2. The resistance R_e decreased proving that the specie motion is enhanced when the temperature was increased. By plotting the conductivities of electrolytes versus the adimensional temperature $\theta = T(K)/T_m(K)$ (T_m : melting temperature expressed in K), the comparison of the electrolyte conductivities within a common scale can be performed (Fig. 6). Two behaviours are well evidenced:

- (i) low conductivities of multi-cation electrolytes;
- (ii) highest conductivities for the all-lithium electrolytes.

In both cases, the values were fairly grouped on a master curve. It also shows clearly that the LiF-LiCl-LiI electrolyte behaves differently from the others. It contains only lithium cation, but it exhibits a conductivity lower than all-lithium electrolytes. Fig. 7 sketches the evolution of the ionic conductivities of electrolytes versus the lithium concentration. A linear dependence is ob-

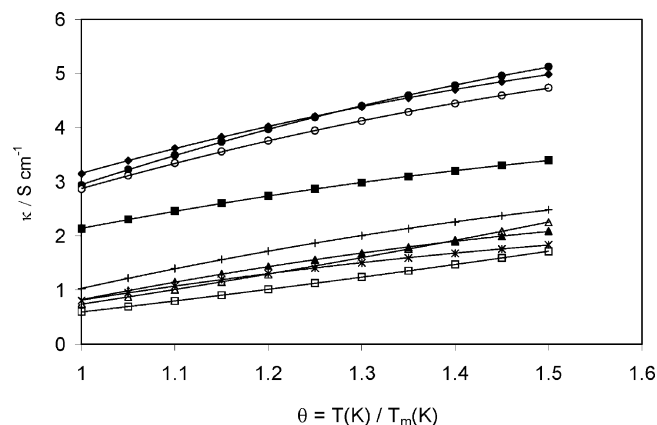


Fig. 6. Evolution of the ionic conductivity vs. the restraint temperature θ ($\theta = T/T_m$) of all electrolytes investigated in this study: (●) LiF-LiCl-LiBr, (◆) LiCl-LiI, (○) LiCl-LiBr-LiI, (■) LiF-LiCl-LiI, (+) LiCl-KCl, (Δ) LiF-LiBr-KBr, (▲) LiCl-LiI-KI, (×) LiI-KI and (□) LiCl-LiBr-KBr.

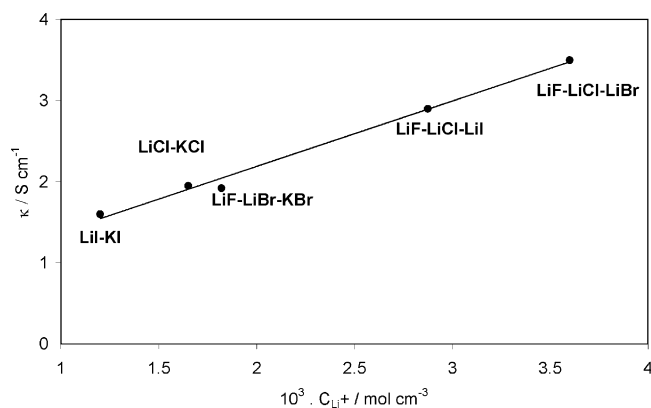


Fig. 7. Evolution of the ionic conductivity of selected electrolytes vs. the molar concentration of lithium cation in the electrolytes.

served. The rather small ionic conductivity of multi-cation electrolytes could be merely ascribed to the low mobility of potassium ions compared to lithium cations. The lower conductivity of the all-lithium electrolyte LiF–LiCl–LiI could be explained by its high density [13] compared to other electrolytes. Moreover, the use of large anion such iodide, could modify the solvation sphere of the lithium cation. Therefore, the effective charge of lithium might be reduced. Molecular dynamic simulation on the solvation. Nevertheless, for thermal battery applications, the LiF–LiCl–LiI electrolyte seems to be attractive. Its melting point is low enough to allow its use for long time functioning and its ionic conductivity is high enough to envisage short time applications with current pulses. The apparent activation energies were extracted from the slope of the curve $\ln \kappa$ versus the inverse of the absolute temperature (Fig. 8). For each electrolyte, straight lines were obtained. The ionic conductivity was expressed as Arrhenius-type expression (Eq. (1)). For iodide-based electrolytes, it was pointed out that activation energy was close to 11 kJ mol^{-1} for multi-cation electrolytes, whereas it was equal to 7 kJ mol^{-1} for all-lithium electrolytes.

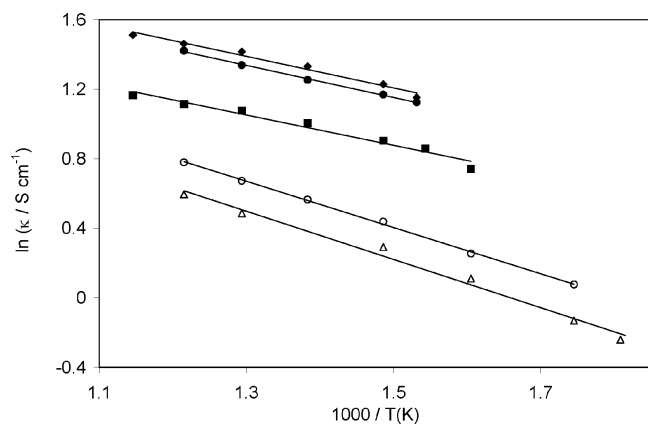


Fig. 8. Evolution of the logarithm of the ionic conductivity vs. the inverse of the absolute temperature of iodide-based electrolytes: (◆) LiCl–LiI, (●) LiCl–LiBr–LiI, (■) LiF–LiCl–LiI, (○) LiCl–LiI–KI and (△) LiI–KI.

4. Conclusions

This work summarises the experimental investigations of ionic conductivity measurements of selected compositions used or envisaged in thermal batteries. It was pointed out that lithium-based compositions present the highest ionic conductivities. It was also shown that some iodide-based electrolytes are suitable to be used in thermal batteries as electrolytes. The LiF–LiCl–LiI eutectic exhibits performances which allow its use as electrolyte in long time operations as well as pulse applications.

Acknowledgements

Patrick Masset expresses his acknowledgements to the following institutions CEA Le Ripault, ASB-Aerospatiale Batteries and LEPMI-INP Grenoble, for providing facilities and their financial support through a Ph.D. grant under a CEA-Industry-University thesis contract (C.T.C.I.). Serge Schoeffert from ASB-Aerospatiale Batteries is deeply thanked for its contribution during this project.

References

- [1] R.A. Guidotti, Proceedings of the 27th International Sampe Technical Conference, 1995.
- [2] R.C. Sharma, Y.A. Chang, *Met. Trans. B* 10B (1979) 103.
- [3] W. Burgmann, G. Urbain, M.G. Froberg, *Mem. Sci. Rev. Metall.* 65 (7–8) (1968) 567.
- [4] S. Dallek, B.F. Larrick, *Thermochim. Acta* 95 (1985) 139.
- [5] J.P. Pemsler, R.K.F. Lam, J.K. Litchfield, S. Dallek, B.F. Larrick, B.C. Beard, *J. Electrochem. Soc.* 137 (1) (1990) 1.
- [6] P. Masset, S. Schoeffert, J.-Y. Poinso, J.C. Poignet, Proceedings of the 40th Power Sources Conference, 2002, p. 246.
- [7] W. Borger, D. Kunze, H.S. Panesar, *Prog. Batt. Sol. Cells* 4 (1982) 258.
- [8] P. Masset, J.-Y. Poinso, J.-C. Poignet, *J. Power Sources* 137 (2004) 140.
- [9] L. Redey, R.A. Guidotti, Proceedings of the 37th Power Sources Conference, 1996, p. 255.
- [10] M.E. Melnichack, J.O. Kleppa, *J. Chem. Phys.* 52 (4) (1970) 1790.
- [11] J.-Y. Poinso, M.-H. Poinso, A. Henry, Proceedings of the 39th International Power Sources Conference, 2000, p. 491.
- [12] K. Rudo, P. Hartwig, W. Weppner, *Chim. Miner.* 17 (4) (1980) 420.
- [13] P. Masset, Ph.D. Thesis, National Polytechnic Institute of Grenoble, 2002.
- [14] G.F. Huttig, W. Steudemann, *Wasser. Z. Phys. C* 126 (1–2) (1927) 279.
- [15] M. Manewa, H.P. Fritz, *A. Anorg. Allg. Chem.* 296 (3) (1973) 279.
- [16] W. Voigt, D. Zeng, *Pure Appl. Chem.* 74 (10) (2002) 1909.
- [17] R.A. Guidotti, F. Reinhardt, ECS Meeting, Philadelphia, 2002.
- [18] L. Redey, M. McParland, R.A. Guidotti, Proceedings of the 34th International Power Sources Conference, 1990, p. 218.
- [19] F.M. Delnick, R.A. Guidotti, *J. Electrochem. Soc.* 137 (1) (1990) 1.
- [20] P. Masset, S. Schoeffert, J.-Y. Poinso, J.-C. Poignet, *J. Power Sources* 139 (2005) 356.
- [21] G.J. Janz, *J. Phys. Chem. Ref. Data* 17 (2) (1988) 309.
- [22] R.C. Vogel, L. Burris, A.V. Tavegaugh, D.S. Webster, E.R. Proud, Argonne National Laboratories, Report ANL-7775, 1970, p. 135.
- [23] D.B. Leiser, O.J. Whittemore Jr., *J. Am. Ceram. Soc.* 50 (1) (1967) 60.
- [24] J. Sangster, A.D. Pelton, *J. Phys. Chem. Ref. Data* 16 (3) (1987) 507.
- [25] C.H. Liu, L.R. Lieto, *J. Chem. Eng. Data* 14 (1) (1969) 83.
- [26] R. Sridhar, C.E. Johnson, E.J. Cairns, *J. Chem. Eng. Data* 15 (2) (1970) 244.

- [27] C.E. Johnson, M.S. Foster, *J. Electrochem. Soc.* 116 (11) (1969) 1612.
- [28] C.E. Johnson, E.J. Hathaway, *J. Electrochem. Soc.* 118 (4) (1971) 631.
- [29] A.G. Bergman, A.S. Arabadshan, *Russ. J. Inorg. Chem.* 8 (5) (1963) 369 (English translation).
- [30] E.W. Yim, M. Feinleib, *J. Electrochem. Soc.* 104 (12) (1957) 622.
- [31] E.W. Yim, M. Feinleib, *J. Electrochem. Soc.* 104 (12) (1957) 626.
- [32] U. Harns, M. Gärtner, A. Schütze, K. Bewilogua, H. Neuhäuser, *Thin Solid Films* 385 (2001) 275.